HTML ABSTRACT + LINKS

Impact of reductive N_2/H_2 plasma on porous low-dielectric constant SiCOH thin films

Hao Cui,[a] Richard J. Carter, and Darren L. Moore
LSI Logic Corporation, 23400 NE Glisan Street, Gresham, Oregon 97030

Hua-Gen Peng and David W. Gidley
Department of Physics, University of Michigan, Ann Arbor, Michigan 48109

Peter A. Burke
LSI Logic Corporation, 23400 NE Glisan Street, Gresham, Oregon 97030

(Received 13 December 2004; accepted 13 April 2005; published online 25 May 2005)

Porous low-dielectric constant (low-κ) SiCOH thin films deposited using a plasma-enhanced chemical-vapor deposition have been comprehensively characterized before and after exposure to a reactive-ion-etch-type plasma of N_2 and H_2 chemistry. The low-κ film studied in this work is a carbon-doped silicon oxide film with a dielectric constant (κ) of 2.5. Studies show that a top dense layer is formed as a result of significant surface film densification after exposure to N_2/H_2 plasma while the underlying bulk layer remains largely unchanged. The top dense layer is found to seal the porous bulk SiCOH film. SiCOH films experienced significant thickness reduction, κ increase, and leakage current degradation after plasma exposure, accompanied by density increase, pore collapse, carbon depletion, and moisture content increase in the top dense layer. Both film densification and removal processes during N_2/H_2 plasma treatment were found to play important roles in the thickness reduction and κ increase of this porous low-κ SiCOH film. A model based upon mutually limiting film densification and removal processes is proposed for the continuous thickness reduction during plasma exposure. A combination of surface film densification, thickness ratio increase of top dense layer to bulk layer, and moisture content increase results in the increase in κ value of this SiCOH film. © *2005 American Institute of Physics*. [DOI: 10.1063/1.1926392]

I. INTRODUCTION

As the critical dimension of very large scale integrated (VLSI) circuits continues to shrink and circuit operating frequency keeps increasing, backend of the line (BEOL) interconnect related issues such as interconnect delay, cross talk noise, and dynamic power consumption become worse. Low-dielectric constant (low-κ) materials are being used as interlayer dielectrics (ILD) in BEOL Cu interconnects to reduce the interconnect capacitance and alleviate these issues.[1,2] SiCOH thin films, which are also commonly referred to as carbon-doped silicon oxide or organosilicate glass, deposited using plasma-enhanced chemical-vapor deposition (PECVD) have gained favor in the VLSI industry as a low-κ ILD due to their relatively robust properties.[3–5] PECVD SiCOH films with a κ of ~3.0 are being widely implemented in BEOL interconnects for 130- and 90-nm nodes. Dielectric films with lower κ values are being actively developed in order to meet the requirements of future generation Cu interconnect technology. This work focuses on a PECVD SiCOH film with κ of 2.5, likely to be used for technology nodes beyond 65 nm. Implementation of porous low-κ ILD materials, however, presents significant process integration and reliability challenges compared to conventional silicon dioxide. Such challenges become more critical as the κ value of the ILD film decreases due to an increase in film porosity. Plasma damage to low-κ films during a photoresist removal ash process has attracted increasing attention as the BEOL critical dimension becomes smaller and the κ value of ILD film decreases. Reactive-ion-etch (RIE)-type oxygen plasma processes have long been used to remove photoresist in VLSI processing. However, SiCOH films have been found to be susceptible to significant oxidative plasma damage.[6–10] As a result, alternative processes including reductive plasma, remotely generated plasma, and wet strip processes have been under investigation for photoresist removal.[11–13] RIE plasmas using reductive gases such as NH_3 and N_2/H_2 have been found to be capable of removing photoresist efficiently with significantly less damage to low-κ SiCOH films than the traditional oxidative plasma. One of the most commonly used methods to further reduce the κ value of dielectric thin films is the introduction of pores into the films. However, porous low-κ SiCOH films also become more sensitive to RIE reductive plasma damage as the film porosity increases. Significant film thickness reduction, κ value increase, and insulating property degradation are among the major consequences of such plasma damage. This work presents a comprehensive study of the impact of RIE-type N_2/H_2 plasma on a PECVD porous SiCOH film with κ of 2.5. Driving forces and mechanisms of thickness reduction and κ increase are proposed and discussed along with changes in other film properties including density, refractive index (RI), chemical bonding structure and composition, surface roughness, and leakage current.

[a]Author to whom correspondence should be addressed; FAX: 503-618-0308; electronic mail: haocui@lsil.com

 © 2005 American Institute of Physics

II. EXPERIMENTAL PROCEDURE

In this work, the effects on PECVD porous SiCOH films with a κ of 2.5 upon exposure to a RIE N_2/H_2 reductive plasma have been studied. Film deposition was achieved using an oxidative–organosilane chemical discharge, with the wafer maintained at 250–300 °C. After deposition, the film was exposed to an ultraviolet (UV) light treatment at ~400 °C to form the oxide network, promote cross-linking in the film, and drive out the porogens, forming a porous film. The final film thickness after deposition and UV treatment was targeted between 6000 and 7000 Å. In order to eliminate any possible low-κ surface skin protection effect and mimic the low-κ trench bottom during dual-damascene processing, all SiCOH films were etched back to ~4000 Å using a $CHF_3/CH_4/N_2$ etch chemistry before N_2/H_2 plasma treatments. A low-temperature, RIE-type plasma of N_2 and H_2 chemistry was used in this study. During the plasma treatment, wafers were maintained at 30 °C in a capacitively coupled chamber with a standard process condition of 50-standard cubic centimeter per minute (SCCM) N_2 and 100-SCCM H_2 gas flows, 40-mTorr chamber pressure, and 1000-W applied rf power. Under these conditions, the removal rate of a photoresist for 193-nm photolithography is measured as ~2600 Å/min.

Film thickness and RI were measured using a spectroscopic ellipsometer system with a wavelength range from 200 to 800 nm. The quoted RI values in this work correspond to a wavelength of 633 nm. A high-precision microbalance with accuracy up to 10^{-4} g was used to monitor the wafer weight change. Positron annihilation lifetime spectroscopy (PALS) was used to study the pore characteristics such as pore size distribution, pore signal intensity, and pore interconnectivity of the SiCOH films before and after the plasma treatments. Chemical composition and its depth profile were determined using Rutherford backscattering spectrometry (RBS), hydrogen forward scattering (HFS) spectrometry, and secondary-ion-mass spectrometry (SIMS). A mercury probe system was used to form metal-insulator-semiconductor (MIS) capacitors and measure the capacitance–voltage ($C-V$) and current-voltage ($I-V$) characteristics of the low-κ SiCOH films at room temperature. The dielectric constant of the films were calculated from the $C-V$ characteristics of the MIS capacitors measured at 500 kHz. The Hg probe system is calibrated using a thermal oxide film to ensure κ measurement accuracy. Chemical bonding structures of these films were investigated from Fourier transform infrared (FTIR) spectroscopy using a BIO-RAD QS-2200 FTIR spectrometer. Transmission spectra at normal incidence were collected at a 4-cm^{-1} resolution. Root-mean-square (rms) surface roughness of SiCOH films was determined from the atomic force microscopy (AFM) images of a 10×10 μm^2 surface area.

III. RESULTS AND DISCUSSION

The impact of a RIE-type reductive N_2/H_2 plasma on a porous SiCOH film with κ of 2.5 has been comprehensively investigated. Film properties such as thickness, refractive index, density, pore characteristics, chemical bonding structure

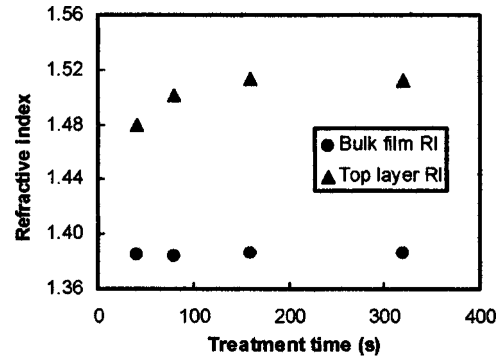

FIG. 1. The refractive index of the top layer and underlying bulk layer of SiCOH film after N_2/H_2 plasma treatment vs treatment time.

and composition, surface roughness, κ, and leakage current have been studied and are presented in the following sections. Mechanisms of N_2/H_2 plasma damage to the SiCOH film including significant thickness reduction and κ increase are proposed and discussed in detail.

A. Thickness, refractive index, and density

A single-layer model was used to successfully measure the thickness and RI of as-deposited and postetch SiCOH films, indicating the homogenous nature of the films. Both films have similar refractive indices of approximately 1.39. However, a dual-layer model, comprising a relatively thin top layer and an underlying bulk layer, was needed to measure films after the N_2/H_2 plasma treatment in order to achieve good fitting between the experimental and simulation data. The necessity of a dual-layer model indicates significant optical property inhomogeneity of the film as a function of thickness. Figure 1 shows the RI of the top layer and underlying bulk layer after N_2/H_2 plasma treatments versus treatment time. The RI of the underlying bulk film remains unchanged compared to the as-deposited film but the top layer is found to have a significantly higher RI. These data suggest that there is significant densification of the surface film after plasma treatment while the bulk film remains relatively unchanged. It is also noted that the RI of the top layer gradually increases with treatment time and tends to saturate at approximately 1.51, indicating a gradual densification of the film surface. The thickness of the top layer formed after N_2/H_2 plasma treatment as a function of treatment time is shown in Fig. 2. The top layer thickness is the highest after 40-s plasma exposure and remains relatively stable from 80- to 320-s treatments. The higher thickness and lower RI of the top layer after 40-s plasma treatment compared to other longer exposure times may indicate incomplete densification of the film surface at that time.

The total film thickness after the N_2/H_2 plasma treatment is calculated from the thickness sum of the top and underlying bulk layers. Significant reduction of the film thickness was observed after the plasma treatment. Figure 3 shows the film thickness reduction as a function of N_2/H_2 plasma exposure time. The film thickness reduction is found to continuously increase with treatment time. The observed reduction in thickness could be due to either film densification (shrinkage), or removal of the film as a result of the

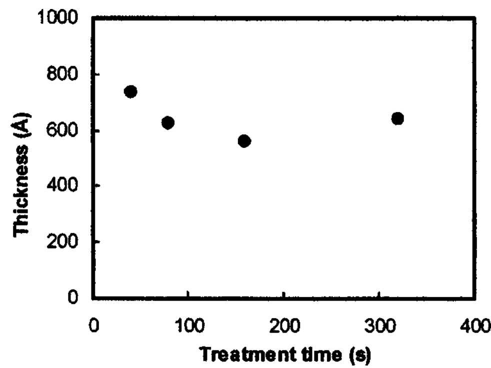

FIG. 2. Thickness of the top layer formed after N_2/H_2 plasma treatment as a function of treatment time.

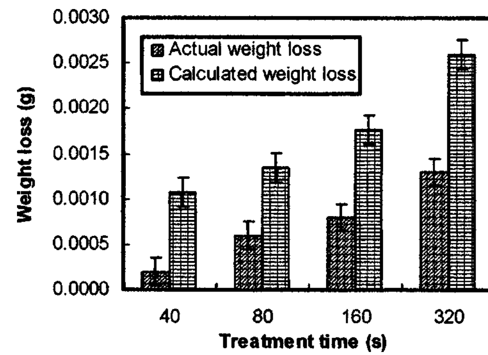

FIG. 4. Wafer weight loss after N_2/H_2 plasma treatment vs treatment time. The expected wafer weight loss assuming no film densification was calculated from the film thickness reduction using a film density of 1.09 g/cm^3.

sputtering effect of plasma ions, or a combination of these two effects. Contributions of film densification and removal to thickness reduction have been studied by monitoring the wafer weight and film density changes. Film densification and removal can both cause film thickness reduction but their effects on film mass loss and density are different. Densification incurs minimal film mass loss thus tends to increase film density. Removal of the film reduces film mass but film density should remain unchanged. By measuring the thickness of an as-deposited film and the wafer weight change before and after deposition, the density of an as-deposited SiCOH film is determined to be 1.09 g/cm^3. All wafers experienced some weight loss after a N_2/H_2 plasma exposure, indicating some degree of film removal. Figure 4 shows the measured wafer weight losses after various N_2/H_2 plasma treatments. Also included is the expected wafer weight loss calculated from the film thickness reduction after plasma treatment using the pristine film density of 1.09 g/cm^3. The calculated weight loss should correlate well with the measured weight loss if film removal is the dominant cause of film thickness reduction. The wafer weight loss continues to increase with treatment time, suggesting that removal of the film plays a significant role and it is a continuous process. The smaller actual wafer weight loss compared to the calculated weight loss indicates that a significant film densification process also occurs during plasma exposure. Compared to longer treatment times, the actual film mass loss after the 40-s plasma treatment is significantly lower than the calculated weight loss. This suggests that densification is more dominant than film removal within this short treatment time.

Assuming the bulk film density remains at 1.09 g/cm^3 after a N_2/H_2 plasma treatment, the density of the top layer can be determined from the wafer weight and individual thickness of the dense surface and bulk layers. Figure 5 shows the top layer density as a function of plasma treatment both before and after a thermal anneal (300 °C in N_2). The significantly higher density of the top layer compared to bulk film again confirms a significant film densification during the plasma exposure. The decrease in top layer density after a thermal anneal is thought to be a result of thermal desorption of moisture content from the film.

The studies of film thickness, RI, and wafer weight loss suggest that film densification and removal due to physical bombardment of the plasma ions both play important roles in the thickness reduction of the porous SiCOH film during a N_2/H_2 plasma treatment. Film densification is suggested to be caused by chemical interactions between plasma ions and chemical bonds in the low-κ film, resulting in pore collapse in the affected region of the film, causing an increase in density. Therefore, the densification rate is greatly affected by the penetration depth of plasma ions into the film. The densification rate is expected to be higher for films with higher porosity due to deeper plasma ion penetration. However, the rate of film densification may be significantly lower when a dense layer starts to form on the surface. The film removal process is thought to be a sputtering effect of the

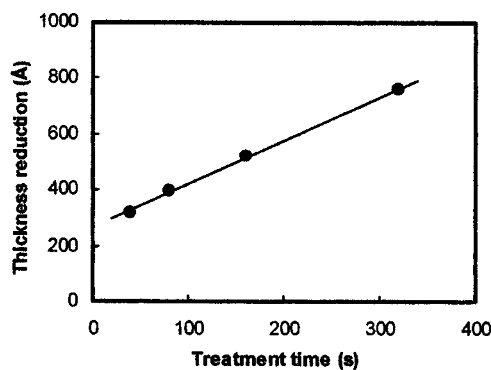

FIG. 3. Thickness reduction of SiCOH after N_2/H_2 plasma treatment as a function of treatment time.

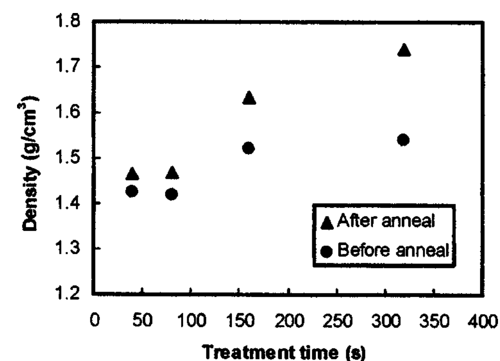

FIG. 5. Density of the top layer after N_2/H_2 plasma treatment as a function of treatment time. Top layer densities measured with and without a thermal anneal at 300 °C in N_2 after plasmas treatment were included.

ions in the plasma. Based upon these results, it is proposed that film densification and removal are two mutually limiting processes causing the SiCOH film thickness reduction during plasma treatment. A model describing the densification and removal sequences during N_2/H_2 plasma treatment is proposed as follows:

(1) There is an immediate surface film densification upon initial exposure to the N_2/H_2 plasma, forming a dense surface layer, thereby minimizing removal of the film during this initial exposure step.
(2) Formation of the dense surface layer impedes further penetration of the plasma ions into the underlying porous bulk film, thereby significantly reducing further film densification.
(3) The dense surface layer is thinned as physical bombardment of the plasma ions becomes more dominant.
(4) As the dense surface layer becomes thinner due to physical bombardment, plasma ions are able to penetrate through the dense layer, causing further film densification.
(5) Repetition of steps 2–4 where an equilibrium between densification and film removal is achieved.

Both densification and physical bombardment processes in the proposed model cause film thickness reduction. The repetition of steps 2–4 leads to a continuous film thickness reduction with plasma treatment time, as shown in Fig. 3. This proposed model suggests that the dense surface layer has a relatively stable thickness as a function of plasma treatment time and a higher RI while the underlying bulk film remains unchanged. Data shown in Figs. 1 and 2 agree with the proposed model. The slight increase in the top dense layer RI with treatment time from 40 to 160 s and the thicker dense surface layer after the 40-s treatment suggest that the densification process is not complete in the first 40 s of the process and progresses further with time. The slight increase in surface layer density with plasma treatment time shown in Fig. 5 also indicates continuous film densification with time.

B. Pore characteristics

PALS is a proven technique in analyzing the pore characteristics of low-κ dielectrics.[14,15] Positronium (Ps) is the bound state of an electron with its antiparticle, positron. PALS utilizes the reduced lifetime of Ps while trapped in open-volume sites to measure the pore size. In this work, PALS analysis was used to investigate the pore characteristics of both the as-deposited SiCOH film and films treated with 40-, 80-, 160-, and 320-s N_2/H_2 plasma time. PALS spectra were acquired with positron implantation energies of 0.55, 1.1, 2.1, 3.1, and 4.1 keV. For a nominal film density of 1.09 g/cm^3, these implantation energies correspond to mean positron implantation depths ($\bar{h}$) of about 10, 29, 82, 155, and 245 nm into the film, respectively. The presence of the top dense layer after N_2/H_2 plasma treatment will result in a slightly shallower positron implantation depth into the films. These different positron implantation energies allow depth-profiling film pore characteristics and studying possible film inhomogeneity.

TABLE I. PALS results of fitting the spectra 50 ns away from the prompt peak. Notice that the vacuum Ps intensity (I_{VAC}) is backscattering subtracted, i.e., positive intensities are the result of Ps diffusing out of the film.

Sample	E (keV)	τ_{PORE} (ns)	I_{PORE} (%)	I_{VAC} (%)
As-dep	0.55	17.8	10.3	6.8
	1.1	17	11.7	2.8
	2.1	15.8	10.8	1.8
	4.1	15.3	12.1	0.6
40-s plasma	0.55	26.7	1.6	0
	1.1	28.2	1.1	0
	2.1	17.6	4.9	0
	3.1	16.3	9.2	0
	4.1	16.8	10.4	0
80-s plasma	0.55	26.2	1.5	0
	1.1	14	2.8	0
	2.1	18.1	6.8	0
	3.1	17.5	11.6	0
	4.1	16.6	14.5	0
160-s plasma	0.55	29.2	1.8	0
	1.1	18.1	1.9	0
	2.1	18.1	8.3	0
	3.1	17.5	11.6	0
	4.1	16.8	15.4	0
320-s plasma	0.55	21.6	1.9	0
	1.1	22.4	1.2	0
	2.1	18.4	8.7	0
	3.1	18.1	13.8	0

First, the part of PALS spectra 50 ns away from the prompt peak is fitted using the widely used spectrum analysis program, POSFIT.[16] This fitting focuses on the Ps lifetime components of large pores (τ_{PORE}) and Ps in vacuum (intrinsic lifetime of ~140 ns) and their intensity (I_{PORE}, I_{VAC}). The results using this fitting method are presented in Table I. By standard definition, pores can be divided into micropores whose diameter is less than 2.0 nm and mesopores if their diameter is greater than 2.0 nm. The 15–18-ns Ps lifetime from the as-deposited and treated films corresponds to spherical pores of 1.6–1.75 nm in diameter. These pores should be considered as micropores. The stable Ps lifetime and fitted intensity (~11%) of these micropores versus implantation energy indicates that the as-deposited film is homogenous. The presence of excess vacuum Ps intensity for the as-deposited film indicates that some Ps formed in the film escape into vacuum, suggesting some degree of pore interconnectivity. In contrast, the N_2/H_2 plasma-treated films show zero Ps escape, indicating a sealed surface after the treatment. At lower positron implantation energies (corresponding to shallower $\bar{h}$), the intensity of large micropores is found to be significantly lower for the plasma-treated films compared to the as-deposited film. All films have similar Ps lifetime and intensity of large micropores at deep implantation depths. This clearly indicates pore collapse and densification in the surface film after plasma treatment while the pore characteristics of the underlying bulk film remains largely unchanged.

To reveal the complete Ps components and intensities, POSFIT was then used to fit the entire spectrum including the

TABLE II. PALS results of fitting the entire spectra. Only the three relevant micropore Ps lifetimes are quoted. The sum of the intensity of the two longer lifetimes, corresponding to the larger pores, is presented in the final column.

Sample	E (keV)	Depth (nm)	τ_1 (ns)	I_1 (%)	τ_2 (ns)	τ_3 (ns)	I_{2+3} (%)
As-dep	1.1	29	2.5	1.1	7.6	13	21
	2.1	82	1.7	4.3	7.3	13.6	19
	4.1	245	0.9	8.2	4.9	13.7	19.7
40-s plasma	1.1	29	1	8	0	9.2	3.7
	2.1	82	1.3	7	7.5	15.3	9.6
	3.1	155	1.1	9	5.6	14.7	15.2
	4.1	245	0.9	9.6	4.9	14.9	17.6
80-s plasma	1.1	29	1.1	5.7	0	9.2	4.1
	2.1	82	1.3	6.9	7.2	15.9	12.3
	3.1	155	1	9.8	5.2	15.7	18.9
	4.1	245	0.9	8.4	5	15.8	20.1
160-s plasma	1.1	29	1.3	3.3	0	9.6	4.5
	2.1	82	1.4	6.4	7.8	16.8	14
	3.1	155	1	9.8	5.2	15.7	18.9
	4.1	245	1	8.4	4.8	16.3	20.1
320-s plasma	1.1	29	1.3	2.1	0	9.6	3.7
	2.1	82	1.4	6.3	7.4	17.7	13.5
	3.1	155	1	8.1	5.2	16.8	19.9
	4.1	245	1	7.9	5.7	17.2	19.5

prompt peak. The three relevant lifetimes associated with Ps in micropores of different sizes and their intensities are presented in Table II. The as-deposited film and treated films all have three Ps lifetimes centered at approximately $\tau_1=1.2$ ns, $\tau_2=6.0$ ns, and $\tau_3=15.0$ ns, respectively. Figure 6 shows the total intensity of pores with two longer micropore Ps lifetime components, I_{2+3}, as a function of $\bar{h}$ for various films. The effect of a surface dense layer is clearly evident from much reduced I_{2+3} at lower implantation depths. The effective thickness of the top dense layer can be estimated from the density-thickness product when the intensity of large micropores reaches half of the bulk film, or approximately 10% intensity in Fig. 6. Assuming a film density of 1.0 g/cm^3, the product of density and thickness of the top dense layer is 130, 95, 80, and 80 nm g/cm^3, respectively, for 40-, 80-, 160-, and 320-s N_2/H_2 plasma exposure time. Using density values of the top dense layer given in Fig. 5, the thickness of the top dense layer is calculated to be 69, 53, 42, and 58 nm, respectively, for treatment times of 40, 80, 160, and 320 s. These values are in reasonably good agreement with those determined from optical measurements.

The pore size distributions (PSDs) of an as-deposited film and the N_2/H_2 plasma-treated films were then deduced using a continuum fitting program, CONTIN, and a hypothesized Ps trapping mechanism.[14,17] Figure 7 compares the PSD of an as-deposited film with the PSD of a film after 40-s plasma treatment with a positron implantation energy of 4.1 keV, which corresponds to deep implantation into the bulk film. Both films have pores ranging in size (spherical diameter model assumed) from about 0.4 to about 2.0 nm with much of the porosity derived from pores with diameter centered around 1.6–1.7 nm. The similar PSD between these two films shows that the pore structure underlying the top dense layer remains largely intact during N_2/H_2 plasma exposure.

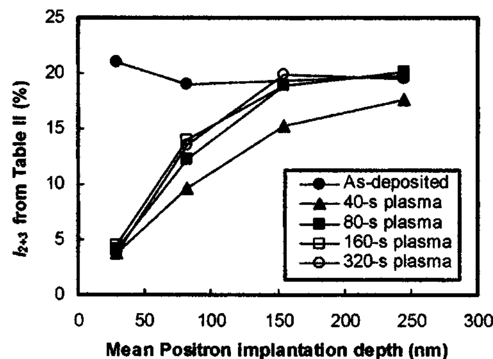

FIG. 6. The intensity of the larger micropores (I_{2+3}) from five-lifetime fitting as a function of mean position implantation depth, given in Table II. The top dense layer thickness can be estimated when intensity I_{2+3} reaches 50% of the undamaged bulk film, or approximately 10%.

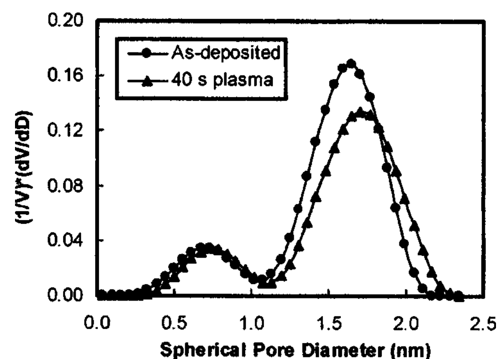

FIG. 7. The pore size distribution of an as-deposited SiCOH film and a film after 40-s N_2/H_2 plasma treatment determined from the continuum spectra fitting.

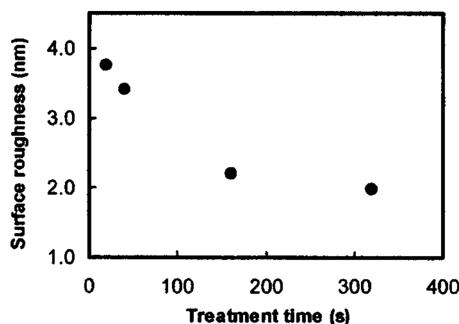

FIG. 8. Root-mean-square surface roughness of SiCOH films after N_2/H_2 plasma treatment vs treatment time.

C. Surface roughness, chemical bonding structure, and chemical composition

Changes in low-κ SiCOH film surface roughness were studied using AFM to characterize the impact of the N_2/H_2 plasma. The as-deposited film has a very smooth surface with a rms surface roughness of 0.41 nm from a 10×10-μm^2 AFM scan. The rms surface roughness increases to 2.72 nm after etch due to the exposure of porous bulk film. Films after etch were then exposed to a N_2/H_2 plasma treatment followed by AFM examination. Figure 8 shows the rms surface roughness of the films after different plasma treatment times. Film surface roughness becomes higher after a 40-s plasma exposure compared to the postetch condition. However, the rms roughness gradually decreases with increasing plasma exposure time. The measured change in surface roughness with plasma treatment time agrees with the proposed model of film densification and removal sequences. The initial increase in surface roughness after 40-s plasma treatment is thought to be caused by nonuniform local film shrinkage during the densification-dominant initial plasma exposure stage. Once the initial dense layer is formed, the densification process slows down while the film removal process due to physical bombardment of the plasma ions becomes more dominant. The physical bombardment process then tends to smooth the film surface by removing the spikes faster than the recessed areas. Figure 8 also indicates that the film surface roughness tends to stabilize as the plasma treatment time increases. It is suggested that as the film densification and removal cycles proceed, an equilibrium between these two mutually limiting processes will be reached and thus the film surface roughness remains relatively unchanged.

Chemical bonding structures of the films before and after N_2/H_2 plasma treatment have been investigated using FTIR. Figure 9 shows the FTIR spectra of films after various processes including deposition, etch only, and etch followed by N_2/H_2 plasma treatments. There is no notable difference between the FTIR spectra of an as-deposited film and a film after etch. The dominant Si–O stretching peak at $\sim 1047\ cm^{-1}$ suggests the Si–O network skeleton of this film. The Si–O shoulder peak at $\sim 1130\ cm^{-1}$ is associated with the Si–O cage structures that are common to porous organosilicate glass-type thin films.[18,19] Peaks of $Si-CH_3$ at $\sim 1274\ cm^{-1}$ and C-H_n stretching at $\sim 2973\ cm^{-1}$ indicate the incorporation of methyl groups in the oxide. The very

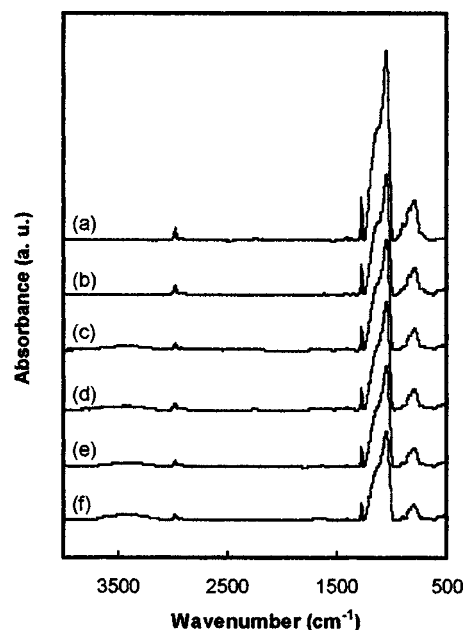

FIG. 9. FTIR spectra of an as-deposited SiCOH film and a film after etch and films after N_2/H_2 plasma treatments.

weak Si–H stretching peak at $\sim 2100\ cm^{-1}$ suggests that most H atoms in the film exist in the form of $C-H_n$ bonds. Peak intensities normalized to the dominant Si–O stretching peak are used in this work to present the relative peak intensities. There are no Si–OH or H–OH peaks in the as-deposited or postetch films, indicating the hydrophobic nature of these films. After N_2/H_2 plasma treatments, the films show distinct differences in FTIR compared to the as-deposited and postetch films. The appearance of a wide peak centered around $3360\ cm^{-1}$ is associated with the Si–OH bond and indicates a significant increase in film moisture content after plasma treatment.

Figure 10 shows the relative Si–OH intensity in the film versus plasma treatment time. The significant increase in moisture content after the N_2/H_2 plasma treatment is thought to be one of the main causes of κ increase, which is discussed in Sec. III D. The relative intensities of $Si-CH_3$ and $C-H_n$ peaks of the films before and after N_2/H_2 plasma treatment are shown in Fig. 11. Lower relative intensities of these two peaks after plasma exposure suggest significant carbon depletion in the affected film. The chemical compo-

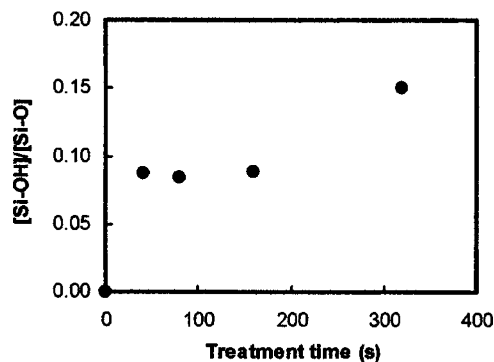

FIG. 10. FTIR [Si–OH]/[Si–O] intensity ratio of SiCOH films after N_2/H_2 plasma treatment vs treatment time.

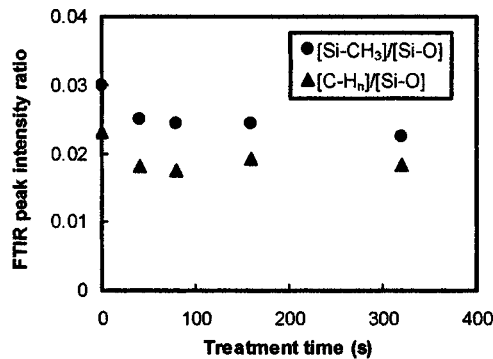

FIG. 11. FTIR $[Si-CH_3]/[Si-O]$ and $[C-H_n]/[Si-O]$ intensity ratios of SiCOH films after N_2/H_2 plasma treatment vs treatment time.

sition of an as-deposited film was determined using RBS and HFS as: 19% Si, 18% C, 31% O, and 32% H. The chemical composition depth profiling of the PECVD SiCOH film after 320-s N_2/H_2 plasma treatment was examined using SIMS. Figure 12 shows the atomic ratio of elements C, O, and H to Si in the film as a function of film thickness. Reduction of C/Si element ratio is clearly seen at the film surface, verifying carbon depletion after N_2/H_2 plasma exposure. Since most H atoms in the film exist in the form of $C-H_n$ bond, a similar reduction in H content would be expected if no external H was introduced into the film. Moisture absorption after plasma treatment and the penetration of H ions from the plasma into the film probably balanced the H loss and maintained the H level in the surface film. The increase of O/Si ratio in the surface film is likely caused by the absorption of moisture into the film as well.

D. Dielectric constant and leakage current

The dielectric constants of the PECVD SiCOH films were determined from the $C-V$ characteristics of MIS capacitors. Both the as-deposited and postetch films have a κ value of 2.5, indicating negligible etch impact on the κ value. Figure 13 shows the κ value of etched films after N_2/H_2 plasma treatments with and without a 300 °C thermal anneal in N_2 before κ measurements. As shown in the figure, κ becomes higher upon exposure to the N_2/H_2 plasma and continues to increase with the exposure time. Such κ increases of the films after N_2/H_2 plasma exposure can be attributed to three main factors:

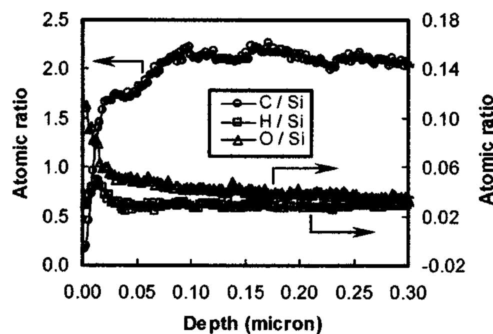

FIG. 12. The atomic ratio of elements C, O, and H, to Si of a SiCOH film after a 320-s N_2/H_2 plasma treatment as a function of film thickness.

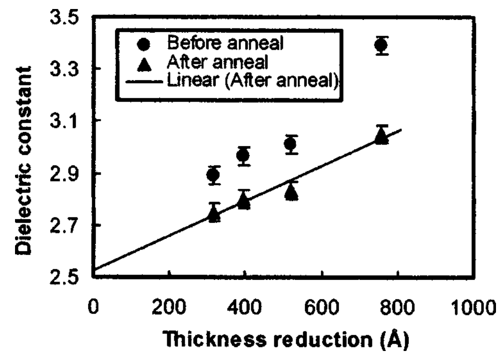

FIG. 13. The dielectric constant of SiCOH films after N_2/H_2 plasma treatments with and without a 300 °C thermal anneal in N_2 right before κ measurements.

(1) formation of a top layer with higher density and κ value,
(2) increasing top dense layer to underlying bulk layer thickness ratio as the densification-removal cycles proceed, and
(3) moisture absorption of plasma-damaged SiCOH film.

Among these factors, the first one can be considered a densification-driven process while the second one can be considered as mainly a physical-bombardment-driven process. As for the first factor, the surface film densification process during plasma exposure creates a top layer with higher density and κ value than the underlying bulk film. The presence of such a top layer makes the overall κ value of the plasma-treated films higher than the as-deposited film. The second factor is more significant for longer plasma treatment time where a significant part of the plasma treatment is in film densification-removal cycles after the initial film densification phase. Once an equilibrium between film densification and removal is reached, the top dense layer thickness remains relatively stable while the underlying bulk film thickness keeps decreasing with treatment time. The overall film κ value increases with the increasing thickness ratio of the top dense layer to the underlying bulk layer. In addition to a higher density, the top dense layer is also chemically altered. The N_2/H_2 plasma attacks the $Si-CH_n$ bonds in the film and creates a considerable amount of dangling bonds, converting the hydrophobic film surface to hydrophilic. As a result, atmospheric moisture diffuses into the damaged SiCOH film and causes the κ value to increase. The significant κ reduction with thermal anneal, as shown in Fig. 13, clearly indicates the contribution of moisture absorption to κ increase.

Of the above three contribution factors to κ increase, the first and second ones are driven by the film densification and removal processes during N_2/H_2 plasma exposure, respectively. Both densification and removal processes directly cause a film thickness reduction. By minimizing the moisture content in the film, thus minimizing the third κ increase factor, there should be a strong correlation between κ increase and film thickness reduction. The κ value and thickness reduction of SiCOH film after N_2/H_2 plasma exposure are compared and presented in Fig. 13. The κ after thermal anneal correlates well with film thickness reduction, where κ increases linearly with thickness reduction. Assuming a lin-

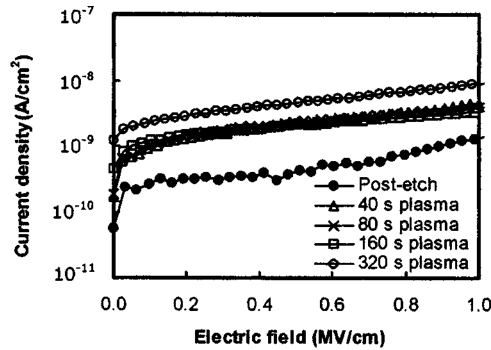

FIG. 14. Current-density–electric-field $(J-E)$ curves of SiCOH films after different N_2/H_2 plasma treatments as compared to a postetch film.

ear fit, κ is found to be very close to 2.5 at zero thickness reduction, further indicating that film densification and removal are the two main driving forces of film κ increase after plasma treatments.

The impact of plasma treatment on film leakage current has been studied by measuring the leakage current of MIS capacitors using a mercury probe system. Figure 14 shows the current-density–electric-field $(J-E)$ characteristics of SiCOH films after plasma treatment compared to a postetch film. No sample received thermal anneal before the leakage current tests. The higher leakage current of plasma-treated films compared to the postetch film indicates significant film insulating property degradation. Moisture content increase in the film after plasma treatment is thought to be the main cause of leakage current increase. The film treated with 320-s plasma shows a significantly higher leakage current than the other plasma-treated films. This is in good agreement with the film moisture content observed from the FTIR spectra shown in Fig. 10.

Film densification and removal processes during N_2/H_2 plasma treatment play key roles in causing film damage such as thickness reduction and κ increase to low-κ SiCOH films. The film removal process, which is caused by the physical bombardment of plasma ions, needs to be minimized for lower damage to the SiCOH film. A lower kinetic energy of plasma ions could help to reduce the physical bombardment effect. Surface film densification, if controlled, could be used as a good pore-sealing technique without significantly damaging the low-κ film. Ideally, a very thin and continuous dense layer can be formed on top of the porous low-κ film with minimal impact on film thickness and κ value. The RIE-type N_2/H_2 plasma studied in this work is shown to be too aggressive, causing significant damage to the porous low-κ film. The film densification processes is mainly driven by the chemical reactions between plasma ions and chemical bonds of the film, while the penetration depth of plasma ions into the film determines the thickness of the dense layer. In addition to reducing the film removal process, a lower kinetic energy of plasma ions can also greatly limit their penetration depth into the low-κ film. One way to significantly reduce the kinetic energy of plasma ions is to reduce or avoid any applied dc bias during plasma treatment that would accelerate the plasma ions towards the wafer. Use of a higher process pressure during plasma treatment can also reduce the kinetic energy of plasma ions. However, photoresist removal efficiency using N_2/H_2 plasma may suffer from a lower kinetic energy of plasma ions. As a result, a balance between low-κ film damage and photoresist removal needs to be considered.

IV. CONCLUSION

RIE-type N_2/H_2 plasma damage to a porous PECVD SiCOH film with a κ of 2.5 has been studied. A dense layer that provides good sealing on top of the underlying porous bulk film, which remains largely intact, is formed after the plasma exposure as a result of surface film densification. The low-κ SiCOH film showed significant damage after plasma exposure including thickness reduction, κ value increase, and leakage current increase accompanied by an increase in density, pore collapse, carbon depletion, and moisture content increase in the top dense layer. Surface film densification and removal processes were found to both play significant roles in SiCOH film damage. A film thickness reduction model including surface film densification and removal as two mutually limiting processes were proposed. Surface densification, moisture absorption, and increasing top dense film to underlying bulk film thickness ratio are identified as the three driving forces for κ increase of the porous SiCOH film upon exposure to reductive N_2/H_2 plasma.

[1] W. Lee and P. Ho, MRS Bull. **22**, 19 (1997).
[2] K. Maex, M. R. Baklanov, D. Shamiryan, F. Iacopi, S. H. Brongersma, and Z. S. Yanovitskaya, J. Appl. Phys. **93**, 8793 (2003).
[3] A. Grill and V. Patel, J. Appl. Phys. **85**, 3314 (1999).
[4] P. Gonon, A. Sylvestre, H. Meynen, and L. V. Cotthem, J. Electrochem. Soc. **150**, F47 (2003).
[5] A. Grill, J. Appl. Phys. **93**, 1785 (2003).
[6] S. Ito, Y. Homma, E. Saski, S. Urichama, and H. Morishima, J. Electrochem. Soc. **137**, 1212 (1990).
[7] E. Kondoh, T. Asano, A. Nakashima, and M. Komatu, J. Vac. Sci. Technol. B **18**, 1276 (2000).
[8] H. Lu, H. Cui, I. Bhat, S. Murarka, W. Lanford, W. Hsia, and W. Li, J. Vac. Sci. Technol. B **20**, 828 (2002).
[9] T. C. Wei, C. H. Liu, J. M. Shieh, S. C. Suen, and B. T. Dai, Jpn. J. Appl. Phys., Part 1 **39**, 7015 (2000).
[10] K. Yonekura, S. Sakmori, K. Goto, M. Matsuura, N. Fujiwara, and M. Yoneda, J. Vac. Sci. Technol. B **22**, 548 (2004).
[11] P. T. Liu *et al.*, J. Electrochem. Soc. **147**, 1186 (2000).
[12] T. C. Chang, P. T. Liu, Y. S. Mor, T. H. Perng, Y. J. Mei, Y. L. Yang, and S. M. Sze, J. Vac. Sci. Technol. B **17**, 2325 (1999).
[13] A. Matsushita *et al.*, Proceedings of 2003 IEEE International Interconnects Technology Conference, Burlingame, CA, 2003, p. 147.
[14] D. W. Gidley, W. E. Frieze, T. L. Dull, J. Sun, A. F. Yee, C. V. Nguyen, and D. Y. Yoon, Appl. Phys. Lett. **76**, 1282 (2000).
[15] J. Sun, D. W. Gidley, T. L. Dull, W. E. Frieze, A. F. Yee, E. T. Ryan, S. Lin, and J. Wetzel, J. Appl. Phys. **89**, 5138 (2001).
[16] W. Puff, Comput. Phys. Commun. **30**, 359 (1983).
[17] S. W. Provencher, Comput. Phys. Commun. **27**, 229 (1982).
[18] R. Almeida and C. Pantano, J. Appl. Phys. **68**, 4225 (1990).
[19] M. Woo, J. Cain, and C. Lee, J. Electrochem. Soc. **137**, 196 (1990).